Spectral properties of hyperbolic nanonetworks with tunable aggregation of simplexes

Marija Mitrović Dankulov,[1,2] Bosiljka Tadić,[2,3] and Roderick Melnik[4,5]

[1]*Scientific Computing Laboratory, Center for the Study of Complex Systems, Institute of Physics Belgrade, University of Belgrade, Pregrevica 118, 11080 Belgrade, Serbia*

[2]*Department of Theoretical Physics, Jožef Stefan Institute, Jamova 39, 1000 Ljubljana, Slovenia*

[3]*Complexity Science Hub Vienna, Josephstadterstrasse 39, 1080 Vienna, Austria*

[4]*MS2Discovery Interdisciplinary Research Institute, M2NeT Laboratory and Department of Mathematics, Wilfrid Laurier University, 75 University Ave W, Waterloo, Ontario, Canada N2L 3C5*

[5]*BCAM–Basque Center for Applied Mathematics, Alameda de Mazarredo 14, E-48009 Bilbao, Spain*

(Received 30 April 2019; published 22 July 2019)

Cooperative self-assembly is a ubiquitous phenomenon found in natural systems which is used for designing nanostructured materials with new functional features. Its origin and mechanisms, leading to improved functionality of the assembly, have attracted much attention from researchers in many branches of science and engineering. These complex structures often come with hyperbolic geometry; however, the relation between the hyperbolicity and their spectral and dynamical properties remains unclear. Using the model of aggregation of simplexes introduced by Šuvakov *et al.* [Sci. Rep. **8**, 1987 (2018)], here we study topological and spectral properties of a large class of self-assembled structures or nanonetworks consisting of monodisperse building blocks (cliques of size $n = 3, 4, 5, 6$) which self-assemble via sharing the geometrical shapes of a lower order. The size of the shared substructure is tuned by varying the chemical affinity ν such that for significant positive ν sharing the largest face is the most probable, while for $\nu < 0$, attaching via a single node dominates. Our results reveal that, while the parameter of hyperbolicity remains $\delta_{\max} = 1$ across the assemblies, their structure and spectral dimension d_s vary with the size of cliques n and the affinity when $\nu \geqslant 0$. In this range, we find that $d_s > 4$ can be reached for $n \geqslant 5$ and sufficiently large ν. For the aggregates of triangles and tetrahedra, the spectral dimension remains in the range $d_s \in [2, 4)$, as well as for the higher cliques at vanishing affinity. On the other end, for $\nu < 0$, we find $d_s \approx 1.57$ independently on n. Moreover, the spectral distribution of the normalized Laplacian eigenvalues has a characteristic shape with peaks and a pronounced minimum, representing the hierarchical architecture of the simplicial complexes. These findings show how the structures compatible with complex dynamical properties can be assembled by controlling the higher-order connectivity among the building blocks.

DOI: 10.1103/PhysRevE.100.012309

I. INTRODUCTION

Controlled self-assembly of nanoparticles with various properties has enabled the engineering of wide classes of materials with new functional features [1]. Among others, the possibilities of designing and assembling three-dimensional (3D) structures of colloidal particles have increased significantly by the discovery of methods for the synthesis of colloids with controlled symmetries and directional interactions [2]. Further possibilities are opened with cooperative self-assembly, where the groups of nanoparticles forming small clusters can join the growing structure [3–7]. These processes utilize a variety of interparticle forces [8], as well as geometry-guided self-assembly [9–11]. By varying the building blocks in different self-assembly processes, the impact of the system's architecture on the emergent functionality in nanostructured materials has been evidenced by experimental investigation, e.g., by the charge transport or spin diffusion, resulting in the enhanced collective dynamics of the assembly [1,4–7,9,12]. On the other side, theoretical investigations of the structure-function interdependence have been greatly facilitated by mapping the assembly onto mathematical graphs or nanonetworks [13]. In this representation, nodes can indicate nanoparticles with their geometrical, physical, and chemical properties, and edges specify the interparticle interaction or chemical bonding often enabled by their physical proximity. This representation allows the use of graph-theory methods to quantify topology and facilitates numerical modeling, as was done, for example, in the study of charge transport by single-electron tunnelings in nanoparticle films [12,14–16], carbon nanotube fillers [17], and others.

On a more global scale, the interplay between the structure and dynamics is captured by spectral properties of networks [18,19]. More specifically, spectral analysis of the adjacency matrix or the Laplacian operator related to the adjacency matrix [20] revealed Fiedler spectral partitioning of the graph and detection of functional modules or mesoscopic communities [21,22], hierarchical organization and homeostatic response [23], the structural changes at the percolation threshold [24], or the occurrence of assortative correlations between nodes [25] and the origin and implications of the degeneracy in network spectra [26,27]. A direct relation between the Laplacian eigenspectrum and the diffusion processes on that network revealed the role of the small-degree nodes and features of the return time of random walks [21,28], as well as the universality of dynamical phase transitions [29] and a deeper understanding of synchronization on complex networks [30]. In this context, the key quantity that relates the structure

to the diffusion and synchronization on a network is the *spectral dimension* [31–33], which can be determined from the properties of the Laplacian spectrum.

The complex functional systems often exhibit a hierarchical architecture and the related hyperbolic geometry. The underlying higher-order connectivity in these structures can be modeled with *simplicial complexes* and describe it with mathematical techniques of the algebraic topology of graphs [34–38]. In this context, simplexes are cliques of different orders $q = 0, 1, 2, 3, \ldots$ representing, respectively, nodes, edges, triangles, tetrahedra, and so on, which are joined into larger-scale structures. Note that a clique of the order q contains cliques of the lower orders up to $q-1$ as its *faces*. The assemblies of cliques can be regarded as topological spaces represented by simplicial complexes. Formally, it holds that in a simplicial complex $\mathcal{K}$, every face of a clique $\sigma \in \mathcal{K}$ also belongs to $\mathcal{K}$, and that a nonempty intersection of two simplexes $\sigma_1, \sigma_2 \in \mathcal{K}$ is a face of both of them. In the context of simplicial complexes, the 1-skeleton consists of nodes and edges, which is the topological graph that is accessible to analysis using standard methods of graph theory. The idea of hierarchical architecture is a center piece in the development of many modern innovative technologies such as 3D printing [39]. In the materials science that motivates our work, such structures are grown by cooperative self-assembly [1,4,6–8,11,40]. Recently, these processes have been modeled by attachments of preformatted objects or simplexes [10,41] under geometric constraints and suitably specified binding rules and parameters. We also draw attention to several other contemporary studies [42–47] that show the importance of simplexes in modeling interactions of higher orders and complex geometry in various physical and biological systems. Whereas in real complex systems whose structure is detectable from experimental data, the corresponding structure can be decomposed into simplicial complexes. For example, in the case of human connectome studied in Refs. [48,49], these simplicial complexes comprise the inner structure of brain anatomical modules. The presence of cliques leading to a hierarchical organization was also found in social networking dynamics [50–52], problems related to traffic dynamics [53], protein-protein interaction networks [23], and so on.

As mentioned above, the hierarchically organized networks possess emergent hyperbolicity or negative curvature in the shortest-path metric, that is, they are Gromov hyperbolic graphs [54–58]. Recently the graphs with a small hyperbolicity parameter δ have been in the focus of the scientific community for their ubiquity in real systems and applications, as well as due to their mathematically interesting structure [55–57,59]. Namely, the upper bound of a small hyperbolicity parameter can be determined from a subjacent smaller graph of a given structure. Generally, it is assumed that both naturally evolving, biological, physical, and social systems develop a negative curvature to optimize their dynamics [42,49,52,60,61]. However, the precise relationship between the hyperbolicity of a network and its spectral and dynamical features remains mostly unexplored.

In this paper, we tackle these issues by systematically analyzing the spectral properties of a class of Gromov 1-hyperbolic graphs, which represent nanonetworks with different architectures of simplicial complexes. Based on the model for the cooperative self-assembly of simplexes introduced in Ref. [41], here we grow several classes of nanonetworks and analyze their topology and spectral properties; the monodisperse building blocks are cliques of the order $n = 3, 4, 5, 6$ while the geometrical compatibility tunes their assembly in the interplay with the varying chemical affinity ν of the growing structure towards the binding group. Specifically, for the negative values of the parameter ν, the effective repelling interaction between the simplexes occurs, while it is gradually attractive for the positive ν. At $\nu = 0$ purely geometrical factors play a role. Our results show that while the hyperbolicity parameter remains constant $\delta = 1$ for all classes, their spectral dimension varies with the chemical affinity ν and the size of the elementary building blocks n. Moreover, these networks exhibit a community structure when the parameter $\nu \geqslant 0$. The inner structure of these communities consists of simplicial complexes with a hierarchical architecture, which manifests itself in the characteristic spectral properties of the Laplacian of the network.

In Sec. II we present details of the model and parameters, while in Sec. III we study different topology features of the considered networks. In Sec. IV we analyze in detail spectral properties of all classes of these networks for varied parameters ν and the size of elementary blocks. Section V is devoted to discussion of the results.

II. SELF-ASSEMBLY OF SIMPLEXES AND THE TYPE OF EMERGENT STRUCTURES

For the growth of different nanonetworks, we use the model rules for the cooperative self-assembly [41,62] with the chemical aggregation of simplexes. Preformatted groups of particles are described by simplexes (full graphs, cliques) of different size $n \equiv q_{\max} + 1$, where $q_{\max}$ indicates the order of the clique. Starting from an initial simplex, at each step, a new simplex is added and attached to the growing network by *docking* along one of its faces, which are recognized as simplexes of the lower order $q = 0, 1, 2, \ldots, q_{\max} - 1$; see online demo [63]. For example, a tetrahedron can be attached by sharing a single node, i.e., a simplex of the order $q = 0$ with the existing network, or sharing an edge, $q = 1$, or a triangle, $q = 2$, with an already existing simplex in the network. The attaching probability depends both on the geometrical compatibility of the q-face of the adding simplex with the current structure as well as on the parameter ν that describes the chemical affinity of that structure towards the addition of new n_a nodes, where $n_a = q_{\max} - q$. More precisely, we have [41]

$$p(q_{\max}, q; t) = \frac{c_q(t) e^{-\nu(q_{\max}-q)}}{\sum_{q=0}^{q_{\max}-1} c_q(t) e^{-\nu(q_{\max}-q)}} \tag{1}$$

for the normalized probability that a clique of the order $q_{\max}$ attaches along its face of the order q. Here $c_q(t)$ is the number of the geometrically similar docking sites of the order q at the evolution time t. Eventually, one of them is selected randomly. By varying the parameter ν from large negative to large positive values, the probability of docking along with a particular face is considerably changed. For example, for the negative values of ν, the growing system "likes" new vertices; consequently, a simplex preferably attaches along a shared vertex

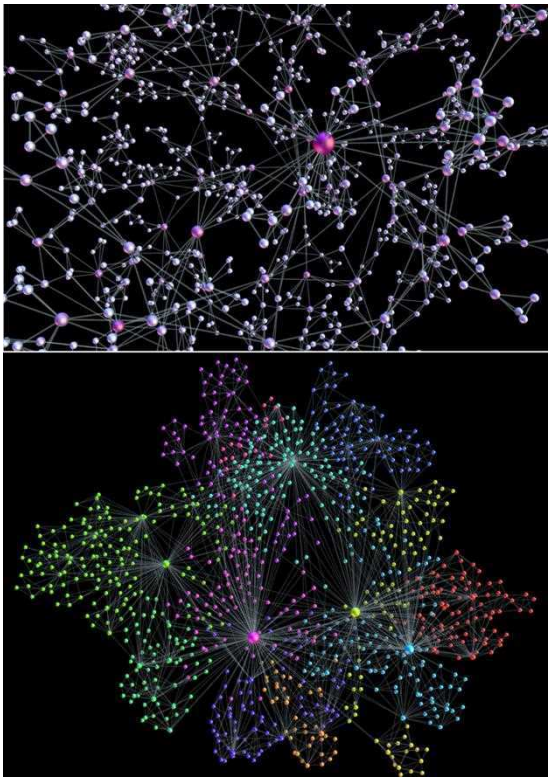

FIG. 1. Aggregates of tetrahedra with strong repulsion, a segment is shown in the top panel, and the case with strong attraction resulting in the network with communities indicated by different colors is shown in the bottom panel.

rather than a larger structure. Effectively, a repulsion between simplexes occurs; see Fig. 1 top. In the other limit, for a large positive ν, the most probable docking is along the potentially largest face, such that an added simplex of the size n shares the maximum number $n-1$ of vertices with the existing structure; see bottom panel in Figs. 1 and 2. Here the simplexes in question experience a strong attraction, which gradually decreases with decreasing ν. For the neutral case $\nu = 0$, the assembly is regulated by strictly geometrical compatibility factors $C_q(t)$, which change over time as the network grows.

In the original model [41], the size of the incoming simplexes is taken from a distribution, whose parameters can be varied. To reveal the impact of the size of these building blocks on the spectral properties of the new structure, here we focus on the networks with *monodisperse* cliques; in particular, we investigate separately the structures grown by aggregation of cliques of the size $n = 3, 4, 5$, and 6 for continuously varied affinity ν. For comparison, we also consider the case with a distribution of simplexes in the range $n \in [3, 6]$. As the examples in Fig. 1 and Fig. 2 show, the structure of the assembly varies considerably with both the size of simplexes and the level of attraction between them. Notice that in the case $n = 2$ the simplex consists of two vertices with an edge between them resulting in a random tree graph. Here $q_{\max} = 1$ and all docking faces are single-vertex sites ($q = 0$). Therefore, the probability $p(1, 0; t) = 1$ is independent of the value of the parameter ν. In this work, we consider networks of different number of vertices $N = 1000$, 5000, and 10 000.

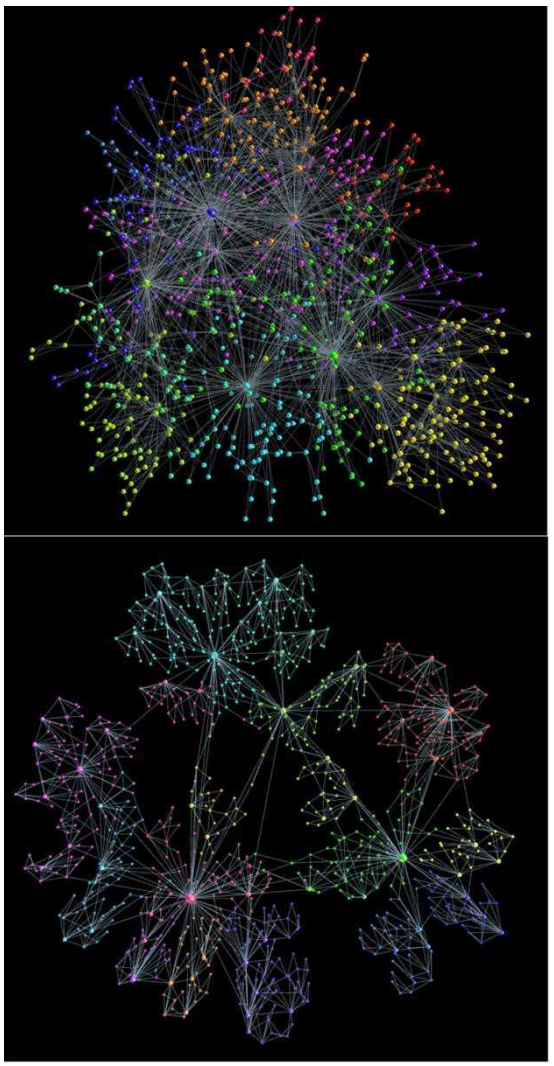

FIG. 2. The networks of the aggregated cliques of mixed sizes $n \in [3, 6]$ distributed according to $\propto n^{-2}$ for $\nu = 5$ (top), and aggregates of triangles for $\nu = 9$ (bottom). The community structure is indicated by different colors of nodes.

III. TOPOLOGICAL PROPERTIES OF THE ASSEMBLED NANONETWORKS

The structure of the assemblies strongly depends on the chemical affinity ν and the size n of the building blocks. For example, a strong repulsion between cliques enables sharing a single node, thus minimizing the geometrical compatibility factor and resulting in a sparse graph (a tree-of-cliques). An example with the tetrahedra as building blocks at $\nu = -9$ is shown in the top panel of Fig. 1. However, for extremally attractive cliques, e.g., for $\nu = 9$, the same building blocks attach mostly via sharing their largest subgraphs (in this case, triangles); thus the geometrical constraints play an important role. This situation results in a dense nanonetwork with a nontrivial community structure, determined by the modularity optimization method [64], as shown in the bottom panel of Figs. 1 and 2. Meanwhile, the modules in the sparse structure can be recognized as the elementary cliques. Notably, the presence of a large clique increases the efficiency of building

TABLE I. Graph measures of the assemblies of cliques of the size n with $N \approx 1000$ vertices for three representative values of the affinity parameter ν: The number of edges E, average degree $\langle k \rangle$, and clustering coefficient $\langle Cc \rangle$, graph's modularity *mod*, diameter D, and ratio of the hyperbolicity parameter $\delta_{\max}$ to $D/2$. Two bottom rows are for mixed clique sizes $n \in [3, 6]$ distributed according to $\propto n^{-\alpha}$.

bb	ν	E	$\langle k \rangle$	$\langle Cc \rangle$	$\langle \ell \rangle$	*mod*	D	$\delta_{\max}/D/2$
$n = 3$	-5	1501	2.999	0.766	9.789	0.928	22	1/11
	0	1734	3.465	0.741	7.265	0.902	16	1/8
	$+5$	1991	3.982	0.735	4.958	0.861	10	1/5
$n = 4$	-5	2009	4.61	0.847	8.718	0.927	19	2/19
	0	2426	4.852	0.808	6.023	0.895	12	1/6
	$+5$	2984	5.968	0.813	3.23	0.715	8	1/4
$n = 5$	-5	2514	5.013	0.878	8.89	0.921	19	2/19
	0	3182	6.351	0.829	5.01	0.856	11	2/11
	$+5$	3997	7.958	0.850	2.703	0.850	5	2/5
$\alpha = 2$	$+5$	2905	5.810	0.820	3.172	0.620	7	2/7
$\alpha = 0$	$+5$	3464	6.298	0.844	2.857	0.569	6	1/3

a nontrivial structure, even for a small attractive potential; cf. Fig. 2 top. We will further discuss the community structure of these networks in connection with their spectral properties in Sec. IV. As explained in the Introduction, we analyze the standard Laplacian operator, which is related to the adjacency matrix of the graph, i.e., a 1-skeleton of the simplicial complex. (A study of combinatorial Laplacians associated with higher-order structures remains out of the scope of this work.) Therefore, we examine the graph's properties that can be related to the Laplacian spectra. In Table I we summarize different graph measures of some monodisperse assemblies whose spectral properties are studied in Sec. IV. We note that the self-assembly process of cliques can result in a broad range of the degree of vertices. Depending on the size of cliques $n \geqslant 3$, several hubs and a power-law tail can appear at the sufficiently strong attraction between them [41]. For illustration, Fig. 3(a) shows the ranking distribution of the degree for several monodisperse assemblies in the case of intense attraction. To get an insight into the structure of the simplicial complexes of these assemblies, we show in Fig. 3(b), how the population f_q of cliques and faces along different topological levels q varies with the size of the building block n. For comparison, we also display f_q in the case of the size $n \in [3, 6]$ distributed as $\sim n^{-\alpha}$ with a small number of larger cliques ($\alpha = 2$) and the statistically similar number of cliques of all sizes ($\alpha = 0$).

As mentioned above, the assemblies of cliques possess a negative curvature in the graph metric space, which implies that they fulfill the Gromov four-point hyperbolicity criterion [54]. More precisely, the graph G is hyperbolic *iff* there is a constant $\delta(G)$ such that for any four vertices (a, b, c, d), the relation $d(a, b) + d(c, d) \leqslant d(a, d) + d(b, c) \leqslant d(a, c) + d(b, d)$ implies that

$$\delta(a, b, c, d) = \frac{d(a, c)+d(b, d)-d(a, d)-d(b, c)}{2} \leqslant \delta(G), \tag{2}$$

where $d(u, v)$ indicates the shortest path distance. Note that the difference in (2) is bounded from above by the minimum distance in the smallest sum $d_{\min} \equiv \min\{d(a, b), d(c, d)\}$. Thus, by plotting $\delta(a, b, c, d)$ against $d_{\min}$ for a large number of 4-tuples, we numerically estimate $\delta(G) \equiv \delta_{\max}$ as the maximum value observed in the entire graph.

As described in Sec. II, the cliques aggregate by sharing their faces, i.e., cliques of a lower order, which leads to some specific properties of the grown structures [41]. In particular, the order of the simplicial complex cannot exceed the order of the largest attaching clique. Moreover, theoretical investigations of these types of structures predict [55–58] that

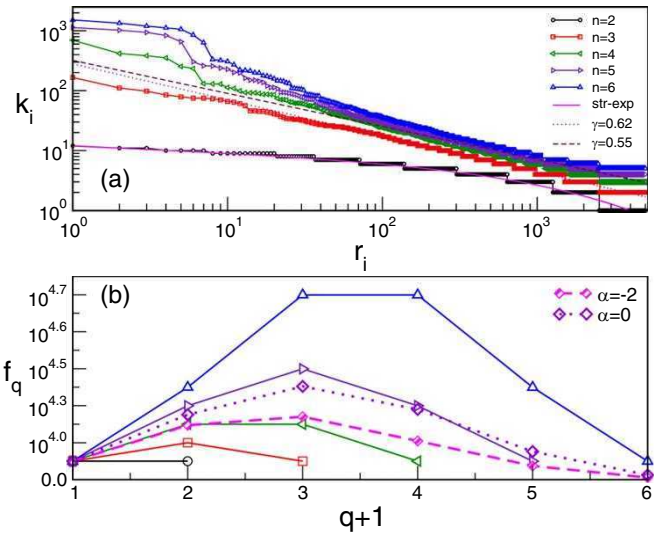

FIG. 3. (a) Ranking distribution of nodes $i = 1, 2, \ldots, 5000$ according to the decreasing degree. The degree k_i of the vertex i is plotted against its rank r_i for different assemblies of cliques of size n, indicated in the legend, and $\nu = 9$. Stretched exponential curve approximates the data for the random tree ($n = 2$), while the asymptotic power-law decay with the exponent γ is appropriate for $n \geqslant 3$. (b) The number of simplexes and faces f_q at different topology level q is plotted against $q + 1$ for the same monodisperse assemblies of the size n as in the top panel (the same legend applies). The additional dotted and dashed lines with diamonds are for the mixed sizes $n \in [3, 6]$ with the distribution $\sim n^{-\alpha}$ and two values of α given in the legend of panel (b).

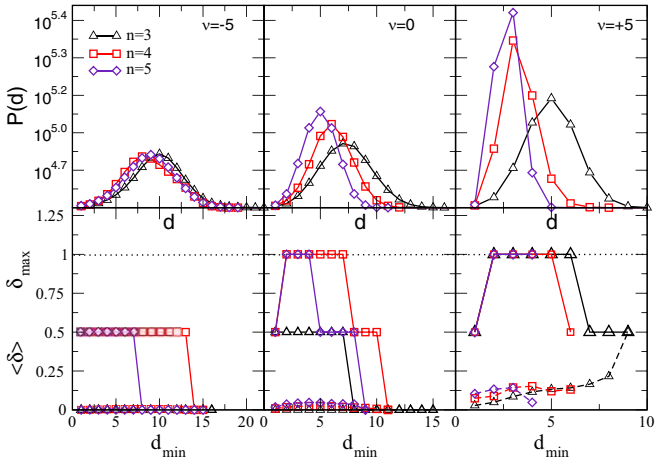

FIG. 4. For the assemblies of simplexes of the size n given in the legend, and three indicated values of the chemical affinity parameter ν. Top panels show the shortest-path distance distributions $P(d)$ vs the distance d. The corresponding bottom panels display the hyperbolicity parameter $\delta_{\max}$ (upper curves, full lines) and $\langle\delta\rangle$ (lower curves, dashed lines) against $d_{\min}$. Thin dotted line indicates the level $\delta_{\max} = 1$.

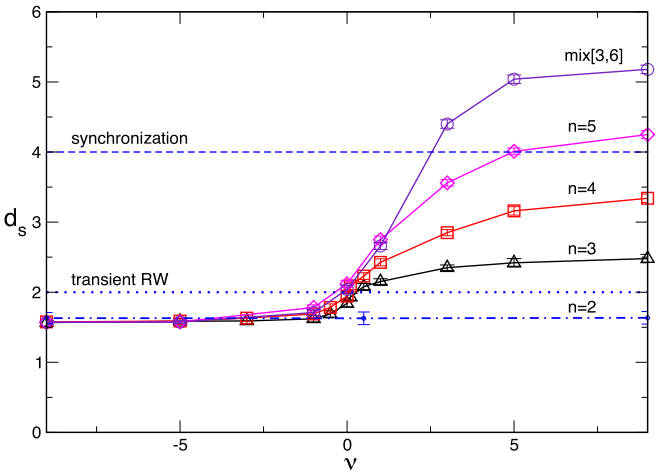

FIG. 5. The lines with different symbols represent the spectral dimension d_s plotted against chemical affinity ν for the aggregates of monodisperse cliques of sizes $n = 3, 4, 5$ and a mixture of cliques of different sizes in the range $n \in [3, 6]$. The bottom line corresponds to the random tree case $n = 2$.

the upper bound of the hyperbolicity parameter of the graph differs from the hyperbolicity of the "atoms" of the structure by at most one unit, that is, $\delta_{\max} = \delta_a + 1$. Given that a clique is ideally hyperbolic (i.e., treelike in the shortest path metric space), we have $\delta_a = 0$, which gives $\delta_{\max} = 1$ for all clique complexes grown by the rules of our model. By sampling up to 10^9 4-tuples of vertices and computing the graph hyperbolicity parameter $\delta(G)$ in Eq. (2), we demonstrate that the hyperbolicity parameter remains $\delta(G) \leqslant 1$ for all studied assemblies. More precisely, while the structure of different assemblies, as well as their distribution of the shortest-path distances, varies with the chemical affinity ν, the upper bound of their hyperbolicity parameter remains fixed in agreement with the theoretical prediction. In Fig. 4 we show the results of the numerical analysis for three representative sets of the assemblies of cliques of different sizes. See also Table I.

IV. SPECTRAL ANALYSIS OF MONODISPERSE ASSEMBLIES

Spectral dimension d_s of a graph, which is defined via $\lim_{t\to\infty} \frac{\log P_{ii}(t)}{\log t} = -\frac{d_s}{2}$, characterizes the distribution of return time $P_{ii}(t)$ of a random walk on that graph [31,65–67]. The diffusion type of processes on network is described by Laplacian operators [21,28]. More precisely, for the undirected graph of N vertices, two diffusion operators are defined, i.e., the Laplacian operator with the components

$$L_{ij} = k_i\delta_{ij} - A_{ij}, \tag{3}$$

and the symmetric normalized Laplacian [68]

$$L^n_{ij} = \delta_{ij} - \frac{A_{ij}}{\sqrt{k_i k_j}}. \tag{4}$$

Here A_{ij} are the matrix elements of the adjacency matrix, k_i is the degree of the node i, and δ_{ij} is the Kroneker symbol. The operators defined with Eqs. (3) and (4) are symmetric and have real non-negative eigenvalues. Both operators have the eigenvalue $\lambda = 0$ with the degeneracy that is equal to the number of connected components in the network. For the networks that have a finite spectral dimension, spectral densities of both Laplacians scale as $P(\lambda) \simeq \lambda^{\frac{d_s}{2}-1}$ for small values of λ. Therefore, the corresponding cumulative distribution $P_c(\lambda)$ scales as

$$P_c(\lambda) \simeq \lambda^{\frac{d_s}{2}}, \quad \lambda \ll 1, \tag{5}$$

and it is suitable [33] for estimating the spectral dimension d_s of the network. Here we analyze the spectral properties of both Laplacian operators (3) and (4) for the networks grown with different building blocks and varied chemical affinity ν; see Figs. 5–7.

We analyze the cumulative spectral density $P_c(\lambda)$ for the Laplacian defined by the expressions (3) and (4) to determine the spectral dimension of the graphs with the adjacency matrix A_{ij}. Note that the spectrum is bounded from below, i.e., $0 \leqslant \lambda$ for all eigenvalues λ. According to Eq. (5), we estimate d_s for each sample by fitting the data of $P_c(\lambda)$ for the values in the range $\lambda \lesssim 0.3$, as illustrated in Fig. 6. The error bars are determined by taking the average from different samples of networks that have 1000 and 5000 nodes. The results summarized in Fig. 5 show how the spectral dimension of the corresponding graphs varies with the chemical affinity ν depending on the size of the elementary building blocks.

As Fig. 5 shows, the impact of the size of the cliques strongly depends on the way that they aggregate, which is controlled by the chemical affinity ν. Precisely, for the sparse structures grown under the considerable repulsion between cliques when $\nu < 0$, we find that the spectral dimension is practically independent of the size of cliques until the repulsion becomes vanishingly weak. In contrast, when $\nu \geqslant 0$ the spectral dimension increases with the size of the elementary cliques. Here the attaching cliques can share their larger faces, thus increasing the impact of the

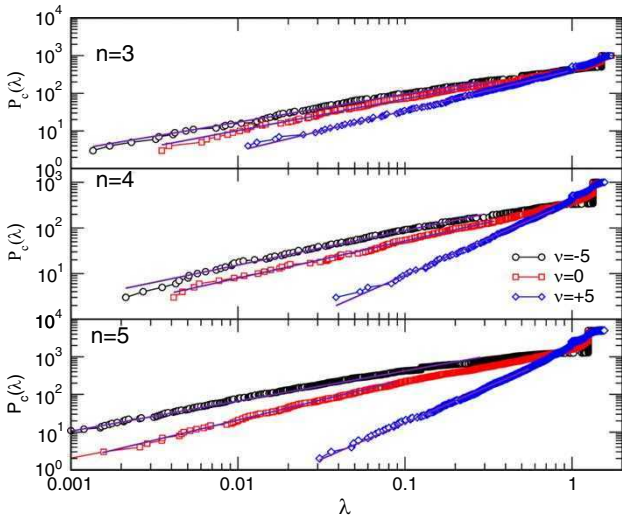

FIG. 6. Several examples of the cumulative spectral density $P_c(\lambda)$ in the range of small λ for the Laplacian operator (4) for the aggregates of triangles (top), tetrahedra (middle), and 5-cliques (bottom). In each panel, three lines in the top-to-bottom order correspond to different values of the chemical affinity $\nu = -5$, 0, and +5, respectively. The corresponding symbol and color for the online version are indicated in the legend.

geometrical compatibility factor. Remarkably, the spectral dimension increases with the strength of the attraction between cliques, which favors sharing increasingly larger faces. These faces are limited by the size of the elementary cliques. More specifically, for all $\nu \geqslant 0$ values, d_s is systematically larger in the aggregates of tetrahedra than those of triangles. In both cases we have that d_s exceeds the limit of the transient random walk, $d_s = 2$, for relatively weak attraction between cliques $\nu \sim 1$. However, both curves remain below $d_s = 4$ for the entire range of ν values. Note that $d_s > 4$ is recognized as the full synchronization condition for the Kuramoto oscillators on network [33], whereas, in the region $d_s \in (2, 4]$, an entrained synchronization with a complex spatiotemporal pattern can be expected [33,69]. Even though a quite compact structure is grown by attaching tetrahedrons via their triangular faces (see bottom panel in Fig. 1), its spectral dimension remains limited as $d_s < 4$, enabling the complex synchronization patterns. We find that the limit $d_s = 4$ can be exceeded when the size of the clique is at least $n = 5$ and the attraction is considerably large, i.e., $\nu \geqslant 5$. In this situation, the agglomerate consists of 5-cliques sharing many tetrahedrons as their largest faces. Interestingly, it suffices to have a few cliques of a large size to grow such agglomerates that cause the spectral dimension $d_s \geqslant 4$. For example, the mixture shown in the top panel of Fig. 2 with $n \in [3, 6]$, where the population of 6-cliques is only 1/4 of the population of 3-cliques, leads to the spectral dimension shown by the top line in Fig. 5. Furthermore, Fig. 6 indicates that not only the spectral dimension but the entire spectrum changes with the size of the cliques and the chemical affinity, as we discuss in more detail in the following.

Next, we determine the spectral density of the normalized Laplacian, defined by (4), by averaging over 10 networks of size $N \approx 1000$ generated for the same values of the model parameters. Note that the eigenvalues of the normalized Laplacian are bounded in the range [21,28] $\lambda_{LN} \in [0, 2]$. In Fig. 7 we show the spectral density of the normalized Laplacian for several representative cases, in particular, for three different aggregates of tetrahedrons corresponding to the strong repulsion, vanishing interaction, and strong attraction, respectively. Also, in panel (e), the spectral distribution is shown for the case of strong attraction $\nu = 9$ for the cliques of different sizes $n \geqslant 3$. It should be noted that iso-spectral structures are observed in the case of the significant repulsion between the cliques $\nu = -9$. In this limit, apart from a structure at small eigenvalues, there is a prominent peak at $\lambda_{LN} = n/(n-1)$, i.e., $\lambda = -1$ in the adjacency matrix, indicating the presence of minimally connected cliques. In contrast, for $\nu \geqslant 0$, the attraction between cliques and the relevance of the geometrical compatibility factors lead to the appearance of larger simplicial complexes. A peak at $\lambda_{LN} = 1$, which is absent in panel (a), starts building at $\nu = 0$, and gradually increases with the increasing ν, as shown in panels (c) and (e). The occurrence of the peak at $\lambda_{LN} = 1$, (i.e., $\lambda = 0$ in the corresponding adjacency matrix [20,26,27]) appears as a characteristic feature of these hyperbolic networks. According to previous studies of scale-free and modular networks [21,28], this peak can be related to the nodes of the lowest degrees in the network. In the present study, such nodes are found in the bottom-right corner of the ranking distribution in Fig. 3(a). Apart from the random tree case, the appearance of this peak reflects the fact that with the increased chemical affinity a broad distribution of degrees occurs with a power-law tail; cf. Fig. 3(a). Notably, the highest peak is when the building cliques are of different sizes $n \in [3, 6]$, compared to the monodisperse structure with $n = 6$. Recently, a more insightful analysis [26,27] revealed different origins of the degeneracy in the adjacency matrix that leads to these two peaks in the spectra. More specifically, this analysis suggests that the occurrence of substructures of nodes, which are equally connected to a surrounding structure in the network, increases the degeneracy of the -1 eigenvalue. Moreover, the reasons for the degeneracy of the 0-eigenvalue were found in the nodes duplication, which is known to characterize the evolution of biological networks, notably demonstrated in analysed protein-protein interaction networks [26,27]. We note that such situations often occur in our model by combining simplexes through their shared faces. The two peaks mentioned above are increasingly more prominent in the case of larger cliques n for $\nu > 0$, where the dominant docking events occur via sharing the largest subclique. Similar spectral properties can be expected for the simplicial complexes grown by different rules, for example, in the models described in Refs. [42–47].

A further exciting feature of these spectral densities is that a characteristic minimum appears between $\lambda_{LN} = 1$ and the structure above it. The results in previous investigations [23] suggest that such minimum in the spectral density is a signature of the hierarchical organization, as demonstrated by an artificial network, which also occurs in the protein-protein interaction network. In the present study, the hierarchical organization of cliques into simplicial complexes occurring at $\nu \geqslant 0$ has been demonstrated by the algebraic topology

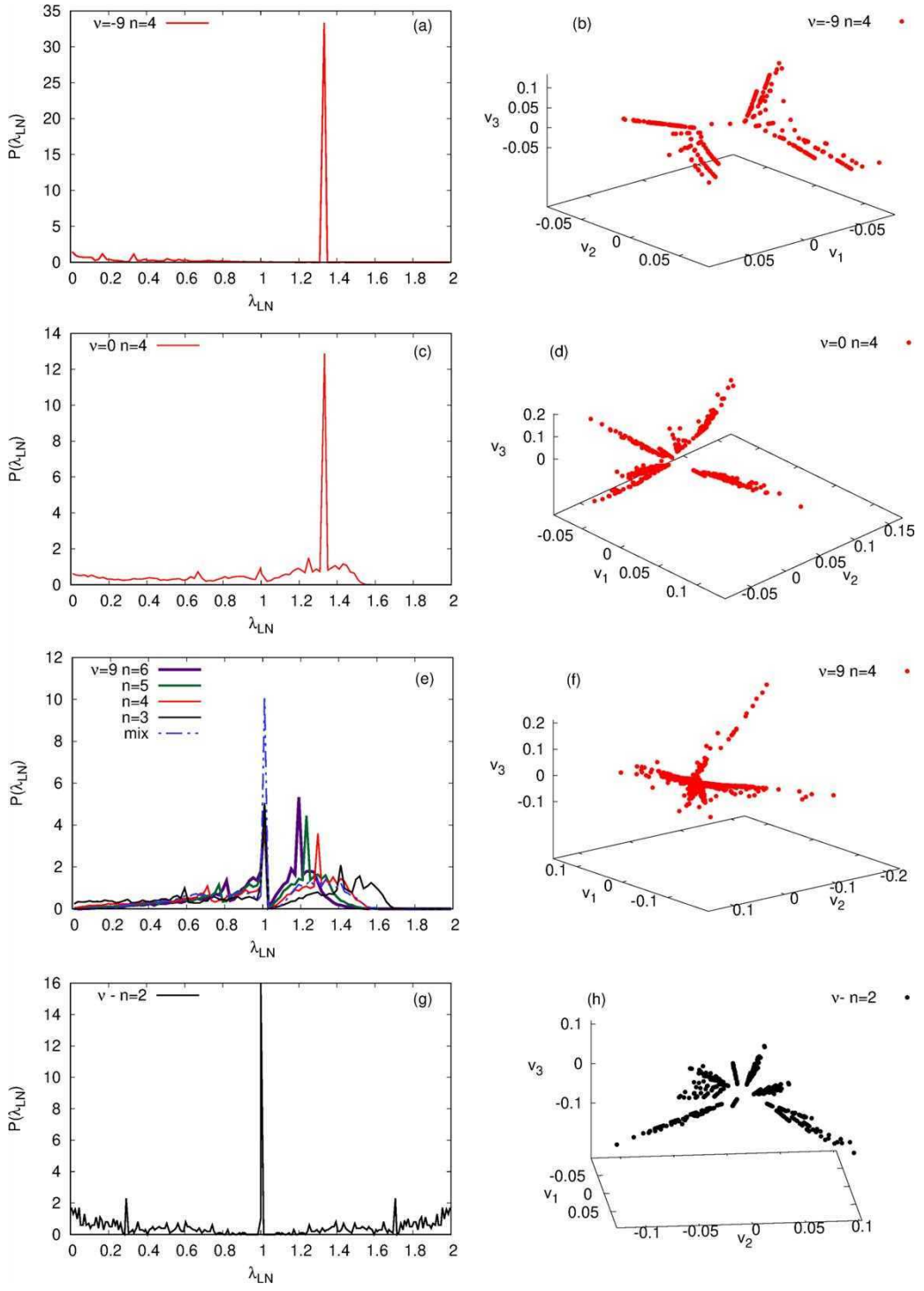

FIG. 7. Spectral distribution (left column) and the corresponding scatter plots of the eigenvectors $v1$, $v2$, $v3$ of the three lowest nonzero eigenvalues of the normalized Laplacian (right column) for the aggregates of tetrahedra $n = 4$ for three different values of the affinity parameter $\nu = -9$ (a, b), $\nu = 0$ (c), (d), and $\nu = +9$ (e), (f). The bottom panels (g) and (h) are for the random tree structure $n = 2$, which is independent of ν. For comparison, we also show the spectra for the cliques of different sizes $n = 3$, 5, and 6, and the mixture $n \in [3, 6]$ in panel (e); the corresponding lines are explained in the legend. The orientation of each 3D plot in panels (b), (d), (f), and (h) is such that it best depicts the number and size of different branches of nonzero components of the corresponding eigenvectors.

methods in Ref. [41]. Here we show by the spectral analysis that these simplicial complexes make the inner structure of mesoscopic communities, which can be identified by the localization of the eigenvectors of the lowest nonzero eigenvalues [21]. In the right column of Fig. 7, panels (b), (d), and (f) show the scatter plot of the three eigenvectors related to the lowest nonzero eigenvalues corresponding to the aggregates of tetrahedrons in the left column. In the limit of strong repulsion between the cliques, the modularity of the entire structure is determined by the original cliques; see Figs. 7(a) and 7(b),

whereas the larger communities with subcommunities appear for $\nu \geqslant 0$ where higher-order connections are increasingly more effective; cf. panels (d) and (f) of Fig. 7. We can expect that similar spectral properties can be found in various real-world networks with the prominent hierarchical organization mentioned in the Introduction. More precisely, the spectra of networks representing functional brain connections, protein-protein interaction networks, as well as various hyperbolic graphs with cliques emerging from the online social dynamics can have features qualitatively similar to the ones discussed above. For completeness, panels (g) and (h) of Fig. 7 show the case $n = 2$, exhibiting the spectral density of a typical random tree structure.

V. DISCUSSION AND CONCLUSIONS

We have studied topological and spectral properties of classes of hyperbolic nanonetworks grown by the cooperative self-assembly. The growth rules [41] that can be tuned by changing the parameter of chemical affinity ν enable us to investigate the role of higher-order connectivity in the properties of the emerging structure. Attaching groups of particles are parameterized by simplexes (cliques) of different sizes which share a geometrical substructure by docking along with the growing network. For the negative values $\nu < 0$, the repulsion among cliques makes them share a single node rather than an edge or a higher structure. On the other hand, $\nu \geqslant 0$ implies that the geometrical factors and the size of the attaching clique become relevant. In particular, the higher positive value of ν implies that a new clique attaches to a previously added clique by sharing its face of the larger order, thus building a more compact structure. Mathematically [58], the attachment of cliques by sharing a face (of any order) leads to simplicial complexes whose hyperbolicity parameter cannot exceed one.

Our results revealed that, while the hyperbolicity parameter remains fixed $\delta_{\max} = 1$ across different assemblies, their topological and spectral properties change with the increased chemical affinity; see Table I and Figs. 5 and 7. Remarkably, the spectral dimension of the structure of strongly repelled cliques of any size is practically indistinguishable from the one of a random tree of the same number of vertices. However, the rest of the spectrum is different from the one of the tree structure; its dominant feature is the presence of cliques as the prominent network modules. On the other hand, the compelling attraction between the cliques for $\nu \gtrsim 0$ results in the spectral dimension that for all sizes $n \geqslant 3$ exceeds the limit $d_s = 2$, compatible with the transient random walk on the network. Further increase of the spectral dimension with the increased affinity parameter ν strongly depends on the size of the cliques. Our results suggest that for a strong attraction with the cliques of size $n \geqslant 5$, the spectral dimension of the network can exceed the limit $d_s = 4$, above which the synchronized phase is expected to exist [33]. However, more interesting structures are grown by smaller cliques or a mixture of different clique sizes with a weak attraction (small positive values of the parameter ν) allowing the sharing a variety of clique's faces. In these cases, we find that the spectral dimension remains in the range of $d_s \in (2, 4]$. These spectral properties are expected to be compatible with an entrained synchronization [33] or a frustrated hierarchical synchronization with intricate spatiotemporal patterns [69]. A detailed analysis of such synchronization patterns on these graphs as well as potentially superdiffusive processes [70] remains for future work. Due to their spectral properties, these structures can be interesting for modeling the complex dynamics in a variety of biological systems and for potential applications. In the framework of the cooperative self-assembly of nanoparticle groups, our analysis shows how the control of the chemical affinity can lead to complex structures with different functional properties. Furthermore, the presented results can be relevant for a deeper understanding of the functional complexity of many important structures with built-in simplicial complexes, such as human connectome [49] and other hierarchically modular networks.

ACKNOWLEDGMENTS

The authors acknowledge the financial support from the Slovenian Research Agency (research code funding number P1-0044) and from the Ministry of Education, Science and Technological Development of the Republic of Serbia, Projects ON171017, and by the Ito Foundation fellowship.

[1] M. A. Boles, M. Engel, and D. V. Talapin, Self-assembly of colloidal nanocrystals: From intricate structures to functional materials, Chem. Rev. **116**, 11220 (2016).

[2] Y. Wang, Yu. Wang, D. R. Breed, V. N. Manoharan, L. Feng, A. D. Hollingsworth, M. Weck, and D. J. Pine, Colloids with valence and specific directional bonding, Nature (London) **491**, 51 (2012).

[3] L. Herkert, A. Sampedro, and G. Fernández, Cooperative self-assembly of discrete metal complexes, Cryst. Eng. Commun. **18**, 8813 (2016).

[4] C. J. Meledandri, J. K. Stolarczyk, and D. F. Brougham, Hierarchical gold-decorated magnetic nanoparticle clusters with controlled size, ACS Nano **5**, 1747 (2011).

[5] D. Toulemon, M. V. Rastei, D. Schmool, J. S. Garitaonandia, L. Lezama, X. Cattoen, S. Begin-Collin, and B. P. Pichon, Enhanced collective magnetic properties induced by the controlled assembly of iron oxide nanoparticles in chains, Adv. Funct. Mat. **26**, 2454 (2016).

[6] Y. Gu, R. Burtovyy, J. Townsend, J. R. Owens, I. Luzinov, and K. G. Kornev, Collective alignment of nanorods in thin Newtonian films, Soft Matter **9**, 8532 (2013).

[7] S. Liu and J. Yu, Cooperative self-construction and enhanced optical absorption of nanoplates-assembled hierarchical Bi2Wo6 flowers, J. Solid State Chem. **181**, 1048 (2008).

[8] D. Luo, C. Yan, and T. Wang, Interparticle forces underlying nanoparticle self-assemblies, Small **11**, 5984 (2015).

[9] A. Hirata, L. J. Kang, T. Fujita, B. Klumov, K. Matsue, M. Kotani, A. R. Yavari, and M. W. Chen, Geometric frustration of icosahedron in metallic glasses, Science **341**, 376 (2013).

[10] S. Ikeda and M. Kotani, Materials inspired by mathematics, Sci. Technology Adv. Mater. **17**, 253 (2016).

[11] B. Senyuk, Q. Liu, E. Bililign, P. D. Nystrom, and I. I. Smalyukh, Geometry-guided colloidal interactions and self-tiling of elastic dipoles formed by truncated pyramid particles in liquid crystals, Phys. Rev. E **91**, 040501(R) (2015).

[12] M. O. Blunt, M. Šuvakov, F. Pulizzi, C. P. Martin, E. Pauliac-Vaujour, A. Stannard, A. W. Rushforth, B. Tadić, and P. Moriarty, Charge transport in cellular nanoparticle networks: Meandering through nanoscale mazes, Nano Lett. **7**, 855 (2007).

[13] J. Živković and B. Tadić, Nanonetworks: The graph theory framework for modeling nanoscale systems, Math. Quantum Nanotechnol. **2**, 30 (2013).

[14] M. Šuvakov and B. Tadić, Modeling collective charge transport in nanoparticle assemblies, J. Phys.: Condens. Matter **22**, 163201 (2010).

[15] M. Šuvakov and B. Tadić, Transport processes on homogeneous planar graphs with scale-free loops, Physica A **372**, 354 (2006).

[16] B. Tadić, M. Andjelković, and M. Šuvakov, The influence of architecture of nanoparticle networks on collective charge transport revealed by the fractal time series and topology of phase space manifolds, J. Coupled Syst. Multiscale Dyn. **4**, 30 (2016).

[17] G.-M. Weng *et al.*, Layer-by-layer assembly of cross-functional semi-transparent MXene-carbon nanotubes composite films for next-generation electromagnetic interference shielding, Adv. Funct. Materials **28**, 1803360 (2018).

[18] C. Castellano and R. Pastor-Satorras, Relating Topological Determinants of Complex Networks to Their Spectral Properties: Structural and Dynamical Effects, Phys. Rev. X **7**, 041024 (2017).

[19] C. Sarkar and S. Jalan, Spectral properties of complex networks, Chaos **28**, 102101 (2018).

[20] J. F. Lutzeyer and A. T. Walden, Comparing graph spectra of adjacency and Laplacian matrices, arXiv:1712.03769.

[21] M. Mitrović and B. Tadić, Spectral and dynamical properties in classes of sparse networks with mesoscopic inhomogeneities, Phys. Rev. E **80**, 026123 (2009).

[22] E. Andreotti, D. Remondini, G. Servizi, and A. Bazzani, On the multiplicity of Laplacian eigenvalues and Fiedler partitions, Linear Algebra Appl. **544**, 206 (2018).

[23] M. A. M. de Aguiar and Y. Bar-Yam, Spectral analysis and the dynamic response of complex networks, Phys. Rev. E **71**, 016106 (2005).

[24] G. Palla and G. Vattay, Spectral transitions in networks, New J. Phys. **8**, 307 (2006).

[25] S. Jalan and A. Yadav, Assortative and disassortative mixing investigated using the spectra of graphs, Phys. Rev. E **91**, 012813 (2015).

[26] A. Yadav and S. Jalan, Origin and implications of zero degeneracy in networks spectra, Chaos **25**, 043110 (2015).

[27] L. Marrec and S. Jalan, Analysing degeneracies in networks spectra, Europhys. Lett. **117**, 48001 (2017).

[28] S. N. Dorogovtsev, A. V. Goltsev, J. F. F. Mendes, and A. N. Samukhin, Spectra of complex networks, Phys. Rev. E **68**, 046109 (2003).

[29] O. Shpielberg, T. Nemoto, and J. Caetano, Universality in dynamical phase transitions of diffusive systems, Phys. Rev. E **98**, 052116 (2018).

[30] A. Arenas, A. Díaz-Guilera, J. Kurths, Y. Moreno, and C. Zhou, Synchronization in complex networks, Phys. Rep. **469**, 93 (2008).

[31] B. Durhuus, T. Jonsson, and J. F. Wheater, The spectral dimension of generic trees, J. Stat. Phys. **128**, 1237 (2007).

[32] I. Seroussi and N. Sochen, Spectral analysis of a non-equilibrium stochastic dynamics on a general network, Sci. Rep. **8**, 14333 (2018).

[33] A. P. Millán, J. J. Torres, and G. Bianconi, Synchronization in network geometries with finite spectral dimension, Phys. Rev. E **99**, 022307 (2019).

[34] R. H. Atkin, From cohomology in physics to q-connectivity in social science, Int. J. Man-Machine Studies **4**, 139 (1972).

[35] P. Gould, Q-analysis, or a language of structure: An introduction for social scientists, geographers, and planners, Int. J. Man-Machine Studies **13**, 169 (1980).

[36] H.-J. Bandelt and V. Chepoi, Metric graph theory and geometry: A survey, in *Surveys on Discrete and Computational Geometry: Twenty Years Later*, Vol. 453, edited by J. E. Goodman, J. Pach, and R. Pollack (Providence, RI: AMS, 2008).

[37] J. Jonsson, *Simplicial Complexes of Graphs*, Lecture Notes in Mathematics Vol. 1928 (Springer-Verlag, Berlin, 2008).

[38] S. Maletić and Y. Zhao, *Simplicial Complexes in Complex Systems: The Search for Alternatives* (Harbin Institute of Technology, Harbin, Peoples Republic of China, 2017).

[39] J. U. Surjadi, L. Gao, H. Du, X. Li, X. Xiong, N. X. Fang, and Y. Lu, Mechanical metamaterials and their engineering applications, Adv. Eng. Mater. **21**, 1800864 (2019).

[40] X. Sun and Y. Q. Ma, Self-Assembly of heterogeneous nano-chain and nano-sheet through the "breaking-to-assembling" route, Ceram. Int. **44**, 23305 (2018).

[41] M. Šuvakov, M. Andjelković, and B. Tadić, Hidden geometries in networks arising from cooperative self-assembly, Sci. Rep. **8**, 1987 (2018).

[42] G. Bianconi and C. Rahmede, Emergent hyperbolic network geometry, Sci. Rep. **7**, 41974 (2017).

[43] G. Bianconi and C. Rahmede, Network geometry with flavor: From complexity to quantum geometry, Phys. Rev. E **93**, 032315 (2016).

[44] O. T. Courtney and G. Bianconi, Weighted growing simplicial complexes, Phys. Rev. E **95**, 062301 (2017).

[45] D. C. da Silva, G. Bianconi, R. A. da Costa, N. S. Dorogovtsev, and J. F. F. Mendes, Complex network view of evolving manifolds, Phys. Rev. E **97**, 032316 (2018).

[46] G. Petri and A. Barrat, Simplicial Activity Driven Model, Phys. Rev. Lett. **121**, 228301 (2018).

[47] N. Cinardi, A. Rapisarda, and G. Bianconi, Quantum statistics in network geometry with fractional flavor, arXiv:1902.10035v1.

[48] B. Tadić, M. Andjelković, B. M. Boshkoska, and Z. Levnajić, Algebraic topology of multi-brain connectivity networks reveals dissimilarity in functional patterns during spoken communications, PLoS ONE **11**, e0166787 (2016).

[49] B. Tadić, M. Andjelković, and R. Melnik, Functional geometry of human connectome and robustness of gender differences, arXiv:1904.03399 [q-bio.NC].

[50] M. Andjelković, B. Tadić, S. Maletić, and M. Rajković, Hierarchical sequencing of online social graphs, Physica A **436**, 582 (2015).

[51] M. Andjelković, B. Tadić, M. M. Dankulov, M. Rajković, and R. Melnik, Topology of innovation spaces in the knowledge networks emerging through questions-and-answers, PLoS ONE **11**, e0154655 (2016).

[52] B. Tadić, Self-organised criticality and emergent hyperbolic networks: Blueprint for complexity in social dynamics, Eur. J. Phys. **40**, 024002 (2019).

[53] M. Andjelković, N. Gupte, and B. Tadić, Hidden geometry of traffic jamming, Phys. Rev. E **91**, 052817 (2015).

[54] J. M. Rodriguez and E. Touris, Gromov hyperbolicity through decomposition of metric spaces, Acta Math. Hungar. **103**, 107 (2004).

[55] S. Bermudo, J. M. Rodríguez, J. M. Sigarreta, and J.-M. Vilaire, Gromov hyperbolic graphs, Discrete Math. **313**, 1575 (2013).

[56] S. Bermudo, J. M. Rodríguez, O. Rosario, and J. M. Sigarreta, Small values of the hyperbolicity constant in graphs, Discrete Math. **339**, 3073 (2016).

[57] A. Martínez-Pérez, Generalized chordality, vertex separators, and hyperbolicity on graphs, arXiv:1708.06153v1.

[58] N. Cohen, D. Coudert, G. Ducoffe, and A. Lancin, Applying clique-decomposition for computing Gromov hyperbolicity, Theor. Comput. Sci. **690**, 114 (2017).

[59] W. Carballosa, D. Pestana, J. M. Rodríguez, and J. M. Sigarreta, Distortion of the hyperbolicity constant in minor graphs, Electron. Notes Discr. Math. **46**, 57 (2014).

[60] W. S. Kennedy, I. Saniee, and O. Narayan, On the hyperbolicity of large-scale networks and its estimation, in *2016 IEEE International Conference on Big Data (Big Data), Washington, DC, December 5–8, 2016* (IEEE, Computer Society, 2016), pp. 3344–3351.

[61] V. Salnikov, D. Cassese, and R. Lambiotte, Simplicial complexes and complex systems, Eur. J. Phys. **40**, 014001 (2018).

[62] M. Šuvakov and B. Tadić, Topology of Cell-Aggregated Planar Graphs, in *International Conference on Computational Science*, edited by V. N. Alexandrov, G. D. van Albada, P. M. A. Sloot, and J. Dongarra, Lecture Notes in Computer Science Vol. 3993 (Springer, Berlin, Heidelberg, 2006), pp. 1098–1105.

[63] M. Šuvakov, M. Andjelković, and B. Tadić, Applet: Simplex aggregated growing graph, http://suki.ipb.rs/ggraph/ (2017).

[64] V. D. Blondel, J.-L. Guillaume, R. Lambiotte, and E. Lefebvre, Fast unfolding of communities in large networks, J. Stat. Mech. (2008) P10008.

[65] R. Rammal and G. Toulouse, Random walks on fractal structures and percolation clusters, J. Phys. Lett. **44**, 13 (1983).

[66] R. Burioni and D. Cassi, Universal Properties of Spectral Dimension, Phys. Rev. Lett. **76**, 1091 (1996).

[67] R. Burioni and D. Cassi, Random walks on graphs: Ideas, techniques, and results, J. Phys. A **38**, R45 (2005).

[68] A. N. Samukhin, S. N. Dorogovtsev, and J. F. F. Mendes, Laplacian spectra of, and random walks on, complex networks: Are scale-free architectures really important, Phys. Rev. E **77**, 036115 (2008).

[69] P. Villegas, P. Moretti, and M. A. Muñoz, Frustrated hierarchical synchronization and emergent complexity in the human connectome network, Sci. Rep. **4**, 5990 (2014).

[70] B. Tadić and S. Thurner, Information superdiffusion on structured networks, Physica A **332**, 566 (2004).